Improving Corrosion Resistance of AZ31B Magnesium Alloy via a Conversion Coating Produced by a Protic Ammonium-Phosphate Ionic Liquid

Hassan H. Elsentriecy, Jun Qu, Huimin Luo, Harry M. Meyer III, Cheng Ma, Miaofang Chi

PII: S0040-6090(14)00806-2
DOI: doi: 10.1016/j.tsf.2014.08.010
Reference: TSF 33632

To appear in: *Thin Solid Films*

Received date: 23 April 2014
Revised date: 1 August 2014
Accepted date: 8 August 2014

Please cite this article as: Hassan H. Elsentriecy, Jun Qu, Huimin Luo, Harry M. Meyer III, Cheng Ma, Miaofang Chi, Improving Corrosion Resistance of AZ31B Magnesium Alloy via a Conversion Coating Produced by a Protic Ammonium-Phosphate Ionic Liquid, *Thin Solid Films* (2014), doi: 10.1016/j.tsf.2014.08.010

Improving Corrosion Resistance of AZ31B Magnesium Alloy via a Conversion Coating Produced by a Protic Ammonium-Phosphate Ionic Liquid

Hassan H. Elsentriecy[1,2], Jun Qu[1,*], Huimin Luo[3], Harry M. Meyer III[1], Cheng Ma[1], Miaofang Chi[1]

[1]Materials Science and Technology Division, Oak Ridge National Laboratory, TN, USA
[2]Central Metallurgical Research and Development Institute, Cairo, Egypt
[3]Energy and Transportation Science Division, Oak Ridge National Laboratory, TN, USA

Abstract

Magnesium alloys are susceptible to corrosion because of their high reactivity and low electrode potential. The present work introduces a conversion coating using a protic ammonium-phosphate ionic liquid (IL). Initial results on the Mg AZ31B alloy have demonstrated substantially improved corrosion resistance for the IL treatment at 300 °C (IL_300C) compared to the treatment at room temperature. Potentiodynamic polarization analysis of the IL_300C treated Mg surface in a NaCl solution exhibited a strong passivation behavior. No pretreatment is needed and the treated surface morphology is well preserved. Cross-sectional nanostructure examination using transmission electron microscopy and element mapping using energy-dispersive X-ray spectroscopy have revealed the IL_300C conversion coating to be a 70-80 nm thick with a two-layer structure. Further surface chemical analysis using X-ray photoelectron spectroscopy suggested such an IL conversion coating possibly composed of metal oxides, metal phosphates, and carbonaceous compounds.

Keywords: magnesium; corrosion; conversion coating, protic ammonium-phosphate ionic liquid

* P.O. Box 2008, MS-6063, Oak Ridge, TN 37831-6063, Tel: (865) 576-9304, E-mail: qujn@ornl.gov

1. Introduction

Magnesium (Mg) alloys are of growing engineering interest to the aerospace and automotive industries because of their high specific strength and low density. However, Mg alloys have high corrosion susceptibility due to Mg's low Reduction Potential, E° = -2.37 V vs. NHE [1] and thus their use in engineering applications has been limited. The corrosion behavior of Mg alloys has been thoroughly reviewed by Song and Atrens [2-5]. The corrosion damage can be generally categorized into galvanic corrosion, intergranular corrosion, stress corrosion cracking, corrosion fatigue, etc. Corrosion prevention for Mg alloys may be achieved by various coating techniques such as chemical conversion coatings, electro- or electroless metal plating, anodizing, gas-phase deposition processes, organic and organic-inorganic coatings, and hydride coatings [1-8]. Traditional conversion coatings are based on hexavalent chromium compounds, which are currently being phased out due to the associated severe environmental risks. Chromate-free conversion coatings [9] using stannate [10, 11], rare earth elements, aluminum, zirconium, niobium, zinc phosphate, or phosphate permanganate are currently in early stages of development and have been reported to retard corrosion of Mg alloys to various extents. Particularly, phosphate salts are of great interest because of their low environmental risks and good performance in forming conversion coatings for paint preparation of magnesium alloys [12-14].

Ionic liquids (ILs) [15] are, as the name indicates, composed solely of cations and anions (see Fig. 1) instead of neutral molecules. They are primarily used as "green" solvents in chemical synthesis, electrochemistry, and catalysis, due to their ultra-low vapor pressure, non-flammability, high thermal stability, and flexible molecular structures. Very limited research in the recent literature (primarily from Forsyth's group [16-22]) suggests that the corrosion of Mg

alloys may be retarded when the magnesium surfaces were exposed to ILs, either at room temperature [16-20] for an extended period, heated at a moderate temperature (50 °C) [18], or with electrical potential bias [21,22]. It is believed that the improved corrosion resistance was attributed to the formation of a conversion film that is often heterogeneous with substantial buildup adjacent to grain boundaries [19,20]. The conversion film formation mechanisms are, however, not yet fully understood. Three possible mechanisms of IL-Mg interactions were proposed in this literature [19]: (1) physical adsorption by electrostatic attraction of the IL species (anions and cations) and formation of a double layer on the metal surface, (2) the anion of the IL chemically reacts with the metal ions dissolved during the immersion process, and (3) anion and/or cation electrochemically breaking down to new species that then react with the Mg surface. Surface chemical analysis supported the third one while little evidence was observed for the first and second [19].

We hypothesize that the Mg surface conversion coating formed in an IL is a result of a series of chemical reactions involving ion breakdowns with the decomposition products reacting with the metal surface. Furthermore, we believe that the conversion coating formation is not limited to electrochemical processes suggested in [19] but can be excited by other energy forms as well, such as thermal and/or mechanical stresses. This was in part inspired by observations in our previous research in IL lubrication, in which we revealed that IL ions tend to break down under the thermal (frictional heating) and mechanical (normal and shear) stresses and then react with the metallic surfaces to form protective boundary films during the wear process [23,25]. These findings have led us to study the application of ILs to the Mg surface at an elevated temperature to form a conversion coating for corrosion protection. The thermal stress is expected to promote a more effective conversion coating formation compared to previous work that involves extended

ILs exposure at either room or mild (50 °C) temperature [11-15]. In our initial effort [26], an **aprotic** IL, tetraoctylammonium di(2-ethylhexyl)phosphate, was used in the conversion treatment at 300 °C, which however required phosphoric acid pickling to activate the Mg surface to gain an effective corrosion protection. One drawback of the pickling process is roughening and discoloring the Mg surface.

Here we present the results of using a **protic** IL trioctylammonium di(2-ethylhexyl)phosphate ($[N_{888}H][DEHP]$) to form an effective anti-corrosion conversion coating for the AZ31B Mg alloy at an elevated temperature with no need of a pretreatment. This may be attributed to the protic ammonium cation of $[N_{888}H][DEHP]$ that readily donates protons (H^+), similar to a weak acid, to activate the Mg surface during the treatment. The protic IL-treated Mg surface had literally no appearance or morphology change. Advanced surface characterization techniques including transmission electron microscopy (TEM), energy-dispersive X-ray spectroscopy (EDS), and X-ray photoelectron spectroscopy (XPS) were used to investigate the IL conversion coating and corrosion protection mechanism.

2. Experimental

2.1. Materials and surface preparation

The Mg alloy used in this study was a wrought AZ31B, kindly provided by Magnesium Elektron North America, MENA. Chemical composition of this alloy was determined by inductively coupled plasma atomic emission spectroscopy at DIRATS Laboratories, Westfield, MA, USA, as shown in Table 1.

Block (25.4 mm x 19.05 mm x 6.35 mm) and disk (15 mm diameter x 3 mm thickness) samples were cut and the test surfaces were ground using SiC abrasive paper up to P2400. The samples were then cleaned with acetone and deionized water (DI) and dried with air stream.

The IL used was trioctylammonium di(2-ethylhexyl)phosphate ($[N_{888}H][DEHP]$). As illustrated in Fig. 1, the protic IL was synthesized by neutralization through a combination of equal molar amounts of trioctylamine (2.37 g, 6.69 mmol) and Di (2-ethylhexyl) phosphoric acid (HDEHP, 2.16 g, 6.69 mmol) at room temperature for 2 hours. The mixture became more viscous upon stirring. The water content of the IL was 980 ppm. Mass spectrometry (MS) analysis confirmed the cation and anion chemistry. MS (ESI positive) m/z = 354.41 (calculated 354.41 for $[C_{24}H_{52}N]^+$) and MS (ESI negative), m/z = 321.23 (calculated 321.22 for $[C_{16}H_{34}PO_4]^-$).

Thermogravimetric analysis (TGA) was conducted on $[N_{888}H][DEHP]$ using a TA Instruments TGA-2950 at a 10 °C /min heating rate in both nitrogen and air environment and results are shown in Fig. 2. There is little difference between the two TGA curves and the onset decomposition temperature is ~235 °C.

The Mg alloy surface was treated by applying a layer of $[N_{888}H][DEHP]$ to the sample surface and then heat treated at 300 °C in a furnace for 7 min (denoted as: IL_300C). The treatment temperature 300 ^oC was selected to ensure rapid decomposition of the IL (see the TGA curve in Fig. 2) during the heating process. After the heat treatment, the sample surface was cleaned by ethanol in an ultrasonic cleaner and dried with a stream of air. For comparison, another sample was treated similarly but at room temperature (RT) for 24 hours (denoted as: IL_RT). A third sample heat-treated at 300 °C without application of the IL (denoted as: As polished_300C) to elucidate the role of the IL in changing the corrosion resistance.

2.2. Surface characterization

The morphology and chemical composition of the coated surfaces were characterized using a scanning electron microscope (SEM) with an energy dispersive x-ray (EDS) analysis unit (Hitachi S-4800 Field Emission SEM), cross-sectional transmission electron microscopy (TEM) examination and X-ray photoelectron spectroscopy (XPS) chemical analysis. TEM samples were prepared using a FEI Nova 200 Dual-beam Focused Ion Beam (FIB) System with a Ga source to extract a thin cross-section of the near-surface zone from the IL-treated surface. A carbon film and then a tungsten layer were deposited on the sample surface prior the FIB process to protect the tribo-film. The TEM system was a Hitachi™ HF-3300 TEM/STEM equipped with a Bruker solid state EDS detector. XPS analysis was carried out on a Thermo Scientific K-Alpha XPS instrument. The x-rays used were monochromatic Al-k_α photons and photo-emitted electrons were analyzed with a hemispherical energy analyzer. Wide survey scans were collected from 0 - 1350 eV at a pass energy of 200 eV to determine overall elemental composition. The K-Alpha energy resolution is adequate at a pass energy of 200 eV and is, in fact, the default setting for survey scans (pass energy does not equal resolution). The composition of the survey scan is always checked against the composition determined by narrow region core level spectra as a "double check". Surface compositions were calculated by measuring peak areas of the primary core levels for all elements present and normalizing the peak areas using tabulated sensitivity factors. Depth profiling was done using a 3 kV Ar-ion sputter beam rastered over an area 1× 2 mm. The base pressure in the analysis chamber was about 10^{-9} Pa. All depth profiles were collected using identical ion gun conditions so that profiles can be compared. Previous measurements on standard SiO2 films gave a sputter rate of ~15 nm/min for these ion gun conditions.

2.3. Electrochemical and immersion corrosion tests

Electrochemical corrosion tests were performed using the potentiodynamic polarization technique. In these tests, the alloy samples were polarized at potentials from -300 to +600 mV vs. OCP (open circuit potential) at a scanning rate of 0.166 mV/s in aerated conditions at room temperature. The test solution was 1 wt.% NaCl saturated with $Mg(OH)_2$ (0.25 g/l). Saturated magnesium hydroxide was used to ensure a stable pH value of the solution near the metal surface during the testing process. The pH of the test solution was measured before and after the measurements and it was almost constant (pH = 10.80 ± 0.2) for all electrochemical measurements conducted in this study. A three-electrode electrochemical cell was used. A Pt sheet (25 mm x 25 mm x 0.2 mm) was used as a counter electrode and Ag/AgCl (4M KCl internal solution) as a reference electrode and a disk AZ31B sample with 1 cm^2 exposed area as a working electrode. All electrochemical tests were conducted using a Princeton Applied Research (PARSTAT 4000, Potentiostat/Galvanostat/EIS Analyzer). The sample to be tested was immersed for 30 min in 700 ml of the test solution before starting the experiment. Experiments were repeated three times to ensure reproducibility of the experimental results. The corrosion current densities (I_{corr}) were determined from polarization curves using VersaStudiov2.10.4412. In the software a potential range of ±250 mV vs. OCP was used to determine the I_{corr} (Tafel fit).

To investigate the effect of corrosive solution on the IL conversion film, the sample treated by the IL at 300 °C was immersed in 1 wt.% NaCl saturated with $Mg(OH)_2$ for 4 hours. XPS analysis was conducted on this sample before and after the exposure to the corrosive solution. Table 2 lists the Mg samples investigated in this study.

3. Results and discussion

3.1. Electrochemical corrosion tests

Figure 3a shows representative potentiodynamic polarization curves of the four Mg samples 'As polished', 'As polished_300C', 'IL_RT', and 'IL_300C' in 1 wt.% NaCl saturated with $Mg(OH)_2$. (The curve of the baseline, as-polished AZ31B sample, has been reported in our previous work [26].) To demonstrate the test repeatability, Fig. 3b shows the repeated runs of IL_300C. Tests on other samples had good repeatability as well but detailed results are not shown here. It can be observed that the resistance to pitting corrosion of the Mg surface treated by the protic IL at 300 °C (IL_300C) is significantly higher than that of the untreated (bare) surface (As polished, heat-treated surface without IL (As polished_300C), or IL-treated surface at RT (IL_RT). This was evidenced by the apparent passivation and barrier behavior (i.e. increased polarization potential with almost constant anodic current) for the IL_300C sample. In contrast, such passivation does not exist for As polished or As polished_300C, and is much weaker for IL_RT. Results in Fig. 3a suggest that the thermal stress under the elevated temperature likely promoted the IL decomposition and interactions with the Mg alloy surface to form a conversion coating with enhanced anti-corrosion characteristics. Unlike an aprotic ammonium-phosphate IL that requires acid pickling to activate the Mg surface [26], this protic IL forms an effective conversion film without any pretreatment. This may be attributed to the protic ammonium cations that readily donate protons (H^+), like a weak acid, to activate the Mg surface.

The corrosion parameters deduced from the polarization curves in Fig. 3a are summarized in Table 3. The IL_300C sample had the lowest corrosion current density (indication of lower corrosion rate) among the other tested samples. In addition and most importantly, the IL_300C

sample showed a higher positive pitting potential (E_{pit}) than that of IL_RT sample. The pit nucleation resistance (the resistance to pitting initiation) measured by the difference between pitting potential and corrosion potential (E_{pit} - E_{corr}) evidently indicates that the pitting corrosion resistance of the IL_300C sample is ~5X higher than that of the IL_RT sample. The IL treatment at the elevated temperature resulted in a higher resistance to the corrosion attack of aggressive ions such as Cl^- ions.

3.2. SEM surface morphology examination

Figure 4 presents SEM images of the as polished and IL_300C treated Mg AZ31B surfaces, which clearly show that the conversion treatment using the protic IL did not induce any noticeable change to the surface appearance or morphology. This is another advantage of using a protic ammonium-phosphate IL over an aprotic IL [26] that requires a pickling pretreatment causing a roughened and discolored surface.

3.3. Cross-sectional TEM examination and EDS elemental mapping

Figure 5 shows a cross-sectional TEM image and EDS element maps of the near surface zone of the IL_300C surface. A surface film was discovered in a two-layer (duplex) structure with a total thickness of 70-80 nm. It is likely that the clear-cut interface between the two layers was the original alloy surface before the IL treatment. Both layers are rich in Mg, O, P, and N. The top layer (30-35 nm) was probably formed by the metallic atoms that diffused out of the surface reacting with the decomposed IL species and oxygen. The second layer seems to be a result of reactions between the alloy elements and the IL species and oxygen that diffused into the metal surface.

3.4. XPS surface chemical analysis

To further characterize the conversion coating on the IL_300C surface, XPS chemical analysis was conducted before and after exposure to a corrosion solution, i.e. IL_300C and IL_300C_corr, as defined in Table 2.

Table 4 shows the XPS survey data for the IL_300C and IL_300C_corr samples. The phosphorus content on the IL_300C surface, originated from the IL, indicates interactions occurred between the IL and the alloy surface. The IL_300C surface contains >30 at.% oxygen suggesting considerable oxidation during the coating process. The little P content after the corrosion test (IL_300C_corr) implies that the conversion coating actively interacted with the salt solution and was eventually dissolved during the corrosion process.

The XPS core level spectra of major elements collected from the IL_300C and IL_300C_corr surfaces are shown in Fig. 6. Likely bonding is labeled on each major peak based on [27, 28]. Peaks of Mg, Al, P and O suggest that oxides and phosphates are dominant. The general binding energy of P 2p is in the range of 133-134 eV indicating P-O bonding. (Considering (a) the tabulated values of P-bonding as noted above, and (b) the B.E. given in the literature by most researchers, and (3) the various elements available in this system for bonding to P, it is reasonable to conclude that the P 2p peak at ~134 eV is P bound to O. If P were bound to one of the various metals or C it would be 3-5 eV lower in BE. In this instance, the P 2p BE is easily determined without peak fitting.) The P peak of IL_300C_corr was very low, consistent with Table 4.

The O 1s data in Fig. 6 were core level spectra collected at a pass energy of 50 eV (our normal “work-a-day PE) to get a qualitative assessment of surface chemistry prior to profiling.

Results reflect a mixture of O species that can be related to metal-oxides (Mg-O and Al-O), P-O, and C-O bonding. (The O 1s could be fit with a complex series of overlapping peaks representing various C/O bonds, O-Mg bonds, and O-P bonds. For this study, it was sufficient to observe that the broad, non-distinct O 1s spectrum was at a BE location that corresponded to these various species and the there was ample O for the amounts of Mg, C, P, Al present.)

The C 1s spectrum shows at least three types of C-bonding: C-C at ~284.8 eV, C-O at 285-286 eV, and carbonate (or some other O-C=O type of carbon species) at ~290 eV. For the IL_300C surface, most of the C is present as the "ubiquitous carbon" that is found on most air-exposed metal surfaces (Co/CO2/hydrocarbons, etc) and C-C bound species from the IL. In addition, peak at higher BE (~289 eV) was observed and is attributed to a carbonate species. This feature is widely observed and reported in the literature for Mg and Mg alloys. For the IL_300C_corr surface, the peak maximum shifts to higher BE, indicating more C-O species on this surface. Note that the peaks are normalized to the same height: the total amount of C on the IL_300C_corr surface 62% less that the total amount of C on the IL_300C surface. The main difference is that the ratio of C-C to C-O bonds has decreases on the IL_300C_corr surface. For this study, it was determined that a qualitative assessment was adequate to understand the starting surface.

Based on comparisons to tabulated BE and the literature, the Mg 2p for both the IL_300C and IL_300C_corr surfaces shows primarily MgO (or Mg^{2+}). From the C 1s, it is clear that some Mg-carbonate is also present. The breadth of the O 1s certainly invites the possibility of Mg-hydroxide. The point is, the starting surface is primarily MgO for the IL_300C_corr. Likewise, the IL_300C surface is primarily MgO, but the small feature at ~61 eV indicates that some Mg-metal is present (this feature is a palsmon that is only visible when metallic Mg is present) and

indeed, one can detect a small shoulder on the low BE side of the MgO peak indicating a metal signal.

Al 2p is a very weak signal and suffers further from being in close proximity to another Mg-plasmon feature at slightly lower BE (this plasmon feature is easier to see in the IL_300C spectrum, just as the plasmon was visible in the Mg 2p spectrum).

Chemical composition-depth profiles for IL_300C, IL_300C_corr surfaces were generated using XPS aided by ion-sputtering.Three elements were deconvoluted: Mg, Al, and O, while other elements were plotted as their total signal with no deconvolution. For Mg, two peaks were used, one for Mg metal (which was trivial to identify due to the presence or absence of the plasmon) and another feature we called Mg ion, which was the reminder of the signal and is primarily MgO but certainly has some hydroxide and carbonate. (Note that the small feature at ~61 eV for Mg 2p in Fig. 6 indicates that some Mg-metal is present. This feature is a palsmon that is only visible when metallic Mg is present. Indeed, one can detect a small shoulder on the low BE side of the MgO peak indicating a metal signal.) Because the profile data is acquired at a relatively low resolution (to increase data acquisition speed), detailed peak fitting into closely overlapping features is difficult, at best. Likewise, the Al 2p was deconvoluted into Al ion (primarily Al-oxide) and Al metal. This deconvolution required fitting three features so that the Mg plasmon could be eliminated. The peak separation of the Al ion and Al metal features is wide enough to make their identifications.

Figure 7 shows the composition data for the IL_300C surface up to 800 sec of sputtering. Figure 7b shows the zoomed-in profiles for elements in lower concentrations. The final crater depth was measured to be 186 nm using an optical surface profiler, translating to an average sputtering rate of ~14 nm/min. While it is understood that the sputtering rate may vary at

different depth into the surface, the average sputtering rate is used here to estimate the film thickness. Apparently there is a surface layer rich of P, O, and oxidized metals. The elements seem to be leveled out after 350 sec sputtering, suggesting a maximum film thickness of ~80 nm, which agree well with the TEM observation in Fig. 5.

Mg (ion), Al (ion), and O (O-Mg) all reach their maximum concentrations around 25-35 nm (100-150 sec) deep, where was speculated to be the original alloy surface under TEM (see Fig. 5). This is because, during the treatment process, the rates of chemical reactions were highest at the original alloy surface where the metallic elements, oxygen, and IL elements (e.g., P) are all rich. Inside the conversion coating (<350 sec of sputtering), the ratio of Mg(ion)/O(O-Mg) is higher than one, implying other non-metallic Mg compounds, e.g., $Mg_3(PO_4)_2$, in addition to MgO. Beyond the 350 sec of sputtering, MgO seems to be the sole non-metallic Mg compound. The phosphorus content (primarily metal phosphates as shown in Fig. 6) indicates that the phosphate anions of the IL was actively involved in the conversion film formation. A higher P concentration was observed in the top layer outside the original alloy surface than the second layer inside the original alloy surface. On the other hand, nitrogen was not detected and the role of the ammonium cations of the IL in the conversion film formation is not clear. The existence of multiple carbon bonds (C-C, C-O, and O-C=O) suggests that such conversion coating contains organic or organometallic compounds in addition to inorganic metal oxides and phosphates.

The XPS composition depth profile of the surface after the corrosion exposure test (IL_300C_corr) is shown in Fig. 8. The increased oxygen concentration and longer sputtering time to remove the surface layer imply growing surface oxides and hydroxides when attacked by Cl^- ions in a salt solution [29]. Since the corroded surface was rough and the crater depth could not the precisely determined by surface profiling, the sputtering rate was not available and the

thickness of the corroded surface layer could not be estimated. The phosphorus content was not traceable (<0.1%) after initial ion sputtering and thus is not shown in the composition profile here. This suggests that the corrosive solution fully dissolved the conversion coating during the 4-hr exposure test. It is interesting to observe no Zn in the corroded surface film.

Results of TEM and XPS confirmed the formation of a dense conversion coating on the Mg AZ31B alloy surface and further revealed a two-layer structure and the composition of a mixture of metal oxides, metal phosphates, and some carbonaceous compounds.

4. Conclusions

This study described a conversion coating for the Mg AZ31B alloy using a protic ammonium-phosphate IL at 300 °C, above its onset decomposition temperature, and demonstrated significantly improved corrosion resistance. The weak acidic nature of the protic IL eliminates the need of a pretreatment as required by an aprotic IL and preserves the surface morphology (that is otherwise often altered by pretreatments). Potentiodynamic polarization analysis of the IL_300C treated Mg surface in 1 wt. % NaCl solution saturated with $Mg(OH)_2$ exhibited a much stronger passivation behavior compared to the untreated surface or treated by the same IL at room temperature. Oxidation without IL did not provide any improvement on the corrosion resistance. Results clearly demonstrated that it is the combination of IL chemistry and the heat treatment that produced an effective anti-corrosion conversion. Cross-sectional TEM/EDS examination and XPS chemical analysis revealed that the IL_300C conversion coating is a 70-80 nm thick in a two-layer structure and is composed of metal oxides, metal phosphates, and some carbonaceous compounds. It is believed that the thermal stress during the heat treatment promotes the IL decomposition and the decomposed species then actively reacts

with the alloy surface to produce phosphates and organic/organometallic compounds, which unites together with the growing oxides to form a dense conversion coating.

Acknowledgements

The authors thank Drs. M. P. Brady and G.-L. Song from Oak Ridge National Laboratory (ORNL) for technical discussions and D.W. Coffey from ORNL for TEM sample preparation. Research sponsored by the Laboratory Directed Research and Development Program of Oak Ridge National Laboratory. H. H. Elsentriecy acknowledges the postdoctoral fellowship administered jointly by ORNL and ORISE.

References

[1] B. A. Shaw, Corrosion resistance of magnesium alloys, ASM Handbook, Volume 13A Corrosion: Fundamentals, Testing, and Protection (#06494G), 2003 ASM International, p. 692-696.

[2] G.-L. Song, A. Atrens, Corrosion mechanisms of magnesium alloys, Advanced Engineering Materials 1 (1999) 11-33.

[3] G.-L. Song, A. Atrens, Understanding magnesium corrosion – a framework for improved alloy performance, Advanced Engineering Materials 5 (2003) 837-858.

[4] G.-L. Song, Recent progress in corrosion and protection of magnesium alloys, Advanced Engineering Materials 7 (2005) 563-586.

[5] G.-L. Song, A. Atrens, Recent insights into the mechanism of magnesium corrosion and research suggestions, Advanced Engineering Materials 9 (2007) 177-183.

[6] S.V. Lamaka, M.F. Montemor, A.F. Galio, M.L. Zheludkevich, C. Trindade, L.F. Dick, M.G.S. Ferreira, Novel hybrid sol–gel coatings for corrosion protection of AZ31B magnesium alloy, Electrochimica Acta 53 (2008) 4773-4783.

[7] M. Yekehtaz, F. Sittner, R. Ugas-Carrión, S. Flege, J. Brötz, W. Ensinger, Characterization of protective sol–gel coatings on magnesium based on phenyl-triethoxysilane precursor, Thin Solid Films 518 (2010) 5223-5226.

[8] J. Hu, Q. Li, X. Zhong, L. Li, L. Zhang, Organic coatings silane-based for AZ91D magnesium alloy, Thin Solid Films 519 (2010) 1361-1366.

[9] R. Petro, M. Schlesinger, G.-L. Song, Ionic liquid treatments for enhanced corrosion resistance of magnesium-based substrates, Modern Electroplating, Fifth Ed., Ed: M. Schlesinger and M. Paunovic, 2010, John Wiley & Sons, Inc.

[10] H. H. Elsentriecy, K. Azumi, H. Konno, Improvement in stannate chemical conversion coatings on AZ91 D magnesium alloy using the potentiostatic technique, Electrochimica Acta 53 (2007) 1006-1012.

[11] H. H. Elsentriecy, K. Azumi, H. Konno, Effects of pH and temperature on the deposition properties of stannate chemical conversion coatings formed by the potentiostatic technique on AZ91 D magnesium alloy, Electrochimica Acta 53 (2008) 4267-4275.

[12] M. F. Montemor, A. M. Simoes, M. J. Carmezim, Characterization of rare-earth conversion films formed on the AZ31 magnesium alloy and its relation with corrosion protection, Applied Surface Science 253 (2007) 6922-6931.

[13] M. F. Montemor, A. M. Simoes, M. G. S. Ferreira, M.J. Carmezim, Composition and corrosion resistance of cerium conversion films on the AZ31 magnesium alloy and its relation to the salt anion, Applied Surface Science 254 (2008) 1806-1814.

[14] D. Hawke, D. L. Albright, A phosphate-permanganate conversion coating for magnesium, Metal Finishing 93 (1995) 34-38.

[15] J. D. Holbrey, K. R. Seddon, Ionic liquids, Clean Products and Processes 1 (1999) 223-236.

[16] M. Forsyth, P. C. Howlett, S. K. Tan, D. R. MacFarlane, N. Birbilis, An ionic liquid surface treatment for corrosion protection of magnesium alloy AZ31, Electrochemical and Solid-State Letters 9 (2006) B52-B55.

[17] N. Birbilis, P. C. Howlett, D. R. MacFarlane, M. Forsyth, Exploring corrosion protection of Mg via ionic liquid pretreatment, Surface & Coatings Technology 201 (2007) 4496-4504.

[18] J. Sun, P. C. Howlett, D. R. MacFarlane, J. Lin, M. Forsyth, Synthesis and physical property characterisation of phosphonium ionic liquids based on $P(O)_2(OR)_2^-$ and $P(O)_2(R)_2^-$ anions with potential application for corrosion mitigation of magnesium alloys, Electrochimica Acta 54 (2008) 254-260.

[19] M. Forsyth, W. C. Neil, P. C. Howlett, D. R. Macfarlane, B. R.W. Hinton, N. Rocher, T. F. Kemp, M. E. Smith, New insights into the fundamental chemical nature of ionic liquid film formation on magnesium alloy surfaces, Applied Materials and Interfaces 1 (2009) 1045-1052.

[20] J. Efthimiadis, W. C. Neil, A. Bunter, P. C. Howlett, B. R. W. Hinton, D. R. MacFarlane, M. Forsyth, Potentiostatic control of ionic liquid surface film formation on ZE41 magnesium alloy, ACS Applied Materials and Interfaces 2 (2010) 1317-1323.

[21] P. C. Howlett, T. Khoo, G. Mooketsi, J. Efthimiadis, D. R. MacFarlane, M. Forsyth, The effect of potential bias on the formation of ionic liquid generated surface films on Mg alloys, Electrochimica Acta 55 (2010) 2377-2383.

[22] J.-A. Latham, P. C. Howlett, D. R. MacFarlane, M. Forsyth, Electrochemical reactivity of trihexyl(tetradecyl)phosphonium bis(2,4,4-trimethylpentyl)phosphinate ionic liquid on glassy carbon and AZ31 magnesium alloy, Electrochimica Acta 56 (2011) 5328-5334.

[23] J. Qu, P. J. Blau, S. Dai, H. M. Luo, H. M. Meyer III, J. J. Truhan, Tribological characteristics of aluminum alloys against steel lubricated by imidazolium and ammonium ionic liquids, Wear 267(5-8) (2009) 1226-1231.

[24] J. Qu, M. Chi, H. M. Meyer III, P. J. Blau, S. Dai, H. Luo, Nanostructure and composition of tribo-boundary films formed in ionic liquid lubrication, Tribology Letters 43(2) (2011) 205-211.

[25] J. Qu, D. G. Bansal, B. Yu, J. Howe, H. Luo, S. Dai, H. Li, P. J. Blau, B. G. Bunting, G. Mordukhovich, D. J. Smolenski, Anti-wear performance and mechanism of an oil-miscible ionic liquid as a lubricant additive, ACS Applied Materials & Interfaces 4 (2) (2012) 997-1002.

[26] H. H. Elsentriecy, H. Luo, H. M. Meyer III, L. L. Grado, J. Qu, Effects of pretreatment and process temperature of a conversion coating produced by an aprotic ammonium-phosphate ionic liquid on magnesium corrosion protection, Electrochimica Acta 123 (2014) 58-65.

[27] J. F. Moulder, W. F. Stickle, P. E. Sobol, and K. Bomben (J. Chastain, editor), Handbook of X-ray Photoelectron Spectroscopy 3rd ed. Perkin-Elmer Corporation (Physical Electronics), 1995.

[28] N. Ikeo, Y. Iijima, N. Nimura, M. Sigematsu, T. Tazawa, S. Matsumoto, K. Kojima, and Y. Nagasawa, Handbook of X-ray Photoelectron Spectroscopy, JEOL, 1991.

[29] N. Hara, Y. Kobayashi, D. Kagaya, N. Akao, Formation and breakdown of surface films on magnesium and its alloys in aqueous solutions, Corrosion Science 49 (2007) 166-175.

Tables

Table 1. Chemical composition of AZ31B alloy in wt. %.

Element	Mg	Al	Zn	Mn	Fe	Zr/Nd/Cu/Ni
Wt. %	95.64	3.03	1.06	0.25	0.01	<0.01

Table 2. List of Mg samples.

Surface treatment	Sample code
As polished without treatment	As polished
As polished at 300 °C for 7 minutes (No IL)	As polished_300C
Treated by IL at 300 °C for 7 minutes	IL_300C
IL_300C + 4-hr immersion in 1 wt.% NaCl saturated with $Mg(OH)_2$	IL_300C_corr
Treated by IL at RT for 24 hours	IL_RT

Table 3. Electrochemical corrosion parameters deduced from polarization curves. E_{corr}: corrosion potential; I_{corr}: corrosion current density; E_{pit}: pitting potential; E_{pit}-E_{corr}: pit nucleation resistance.

Sample	E_{corr} (V vs. Ag/AgCl)	I_{corr} ($\mu A/cm^2$)	E_{pit} (V vs. Ag/AgCl)	E_{pit}-E_{corr} (mV vs. Ag/AgCl)
As polished [26]	-1.411	195.843	NA	NA
As polished_300C	-1.479	131.638	NA	NA
IL_300C	-1.437	13.566	-1.31	127
IL_RT	-1.451	25.973	-1.427	24

Table 4. Surface composition (at.%) (survey scan).

	Mg	Al	Zn	O	C	P	N
IL_300C	19.5	0.8	0.0	33.8	41.9	2.9	0.4
IL_300C_corr	34.4	0.6	0.0	48.9	16.0	0.1	0.0

Figure captions

Figure 1. Synthesis scheme and molecular structure of the protic IL [N_{888}H][DEHP].

Figure 2. TGA curves of [N_{888}H][DEHP].

Figure 3. Potentiodynamic polarization curves of (a) comparison of untreated [21] and IL-treated Mg AZ31B alloy measured in 1 wt.% NaCl saturated with $Mg(OH)_2$ and (b) showing good repeatability.

Figure 4. SEM images of Mg AZ31B surfaces before (a) [21] and after (b) IL treatment at 300 °C.

Figure 5. Cross-sectional TEM image and EDS elemental maps of the IL conversion coating (formed at 300 °C) on the Mg AZ31B alloy surface.

Figure 6. XPS core level spectra of IL_300C treated surfaces before (blue) and after (red) the 4-hr exposure corrosion test.

Figure 7. XPS composition depth profile of the IL_300C treated surface before corrosion testing; 7b showing the zoomed-in profiles for elements in lower concentrations.

Figure 8. XPS composition depth profile of the IL_300C treated surface after the 4-hr exposure corrosion test (IL_300C_corr); 8b showing the zoomed-in profiles for elements in lower concentrations.

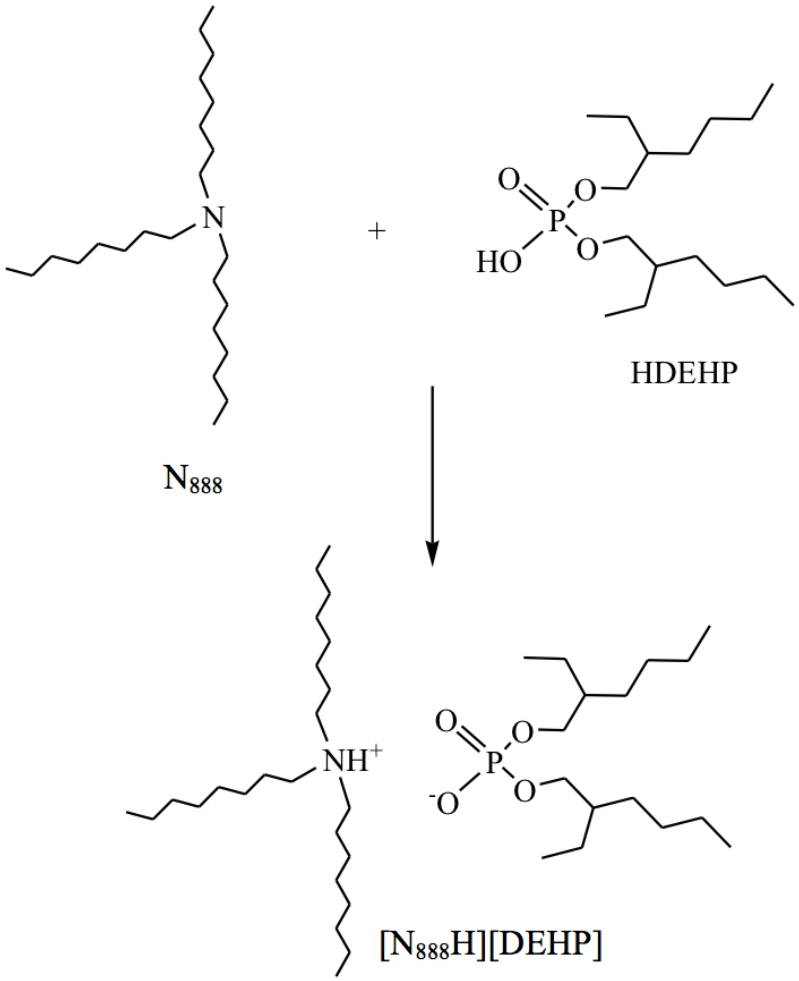

Figure 1. Synthesis scheme and molecular structure of the protic IL $[N_{888}H][DEHP]$.

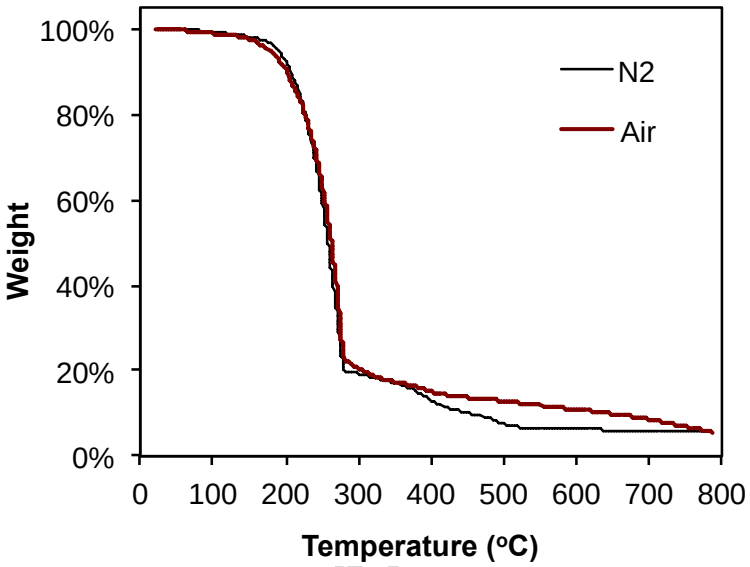

Figure 2. TGA curves of $[N_{888}H][DEHP]$.

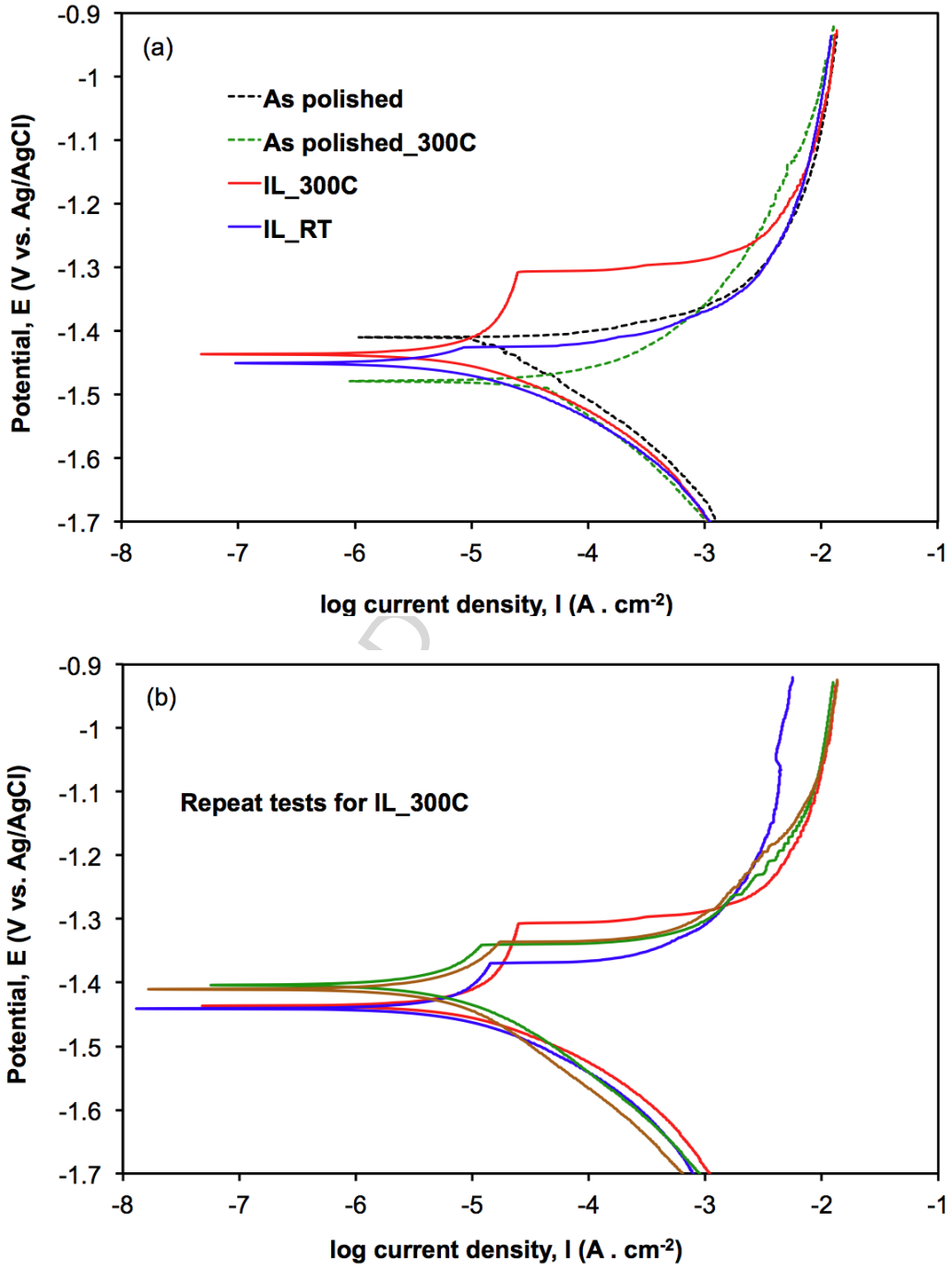

Figure 3. Potentiodynamic polarization curves of (a) comparison of untreated [21] and IL-treated Mg AZ31B alloy measured in 1 wt.% NaCl saturated with $Mg(OH)_2$ and (b) showing good repeatability.

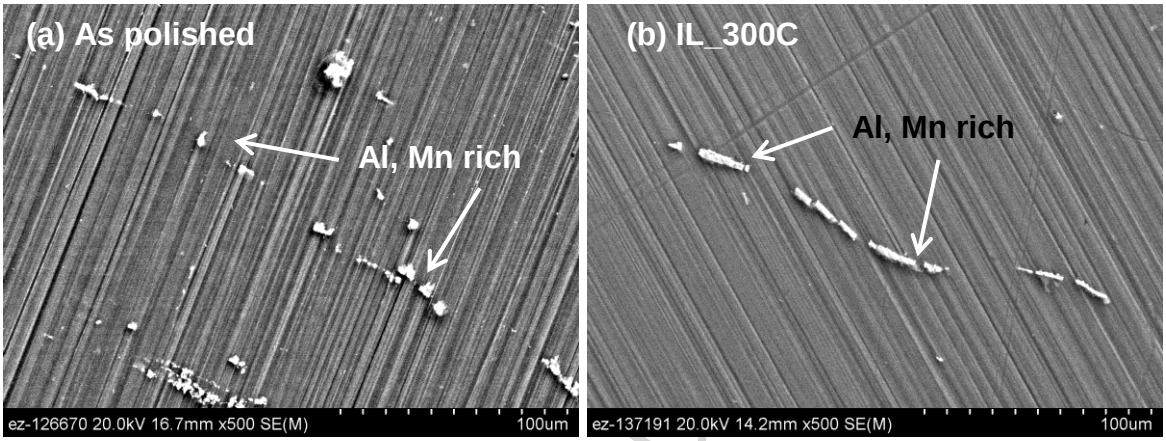

Figure 4. SEM images of Mg AZ31B surfaces before (a) [21] and after (b) IL treatment at 300 °C showing little morphology change.

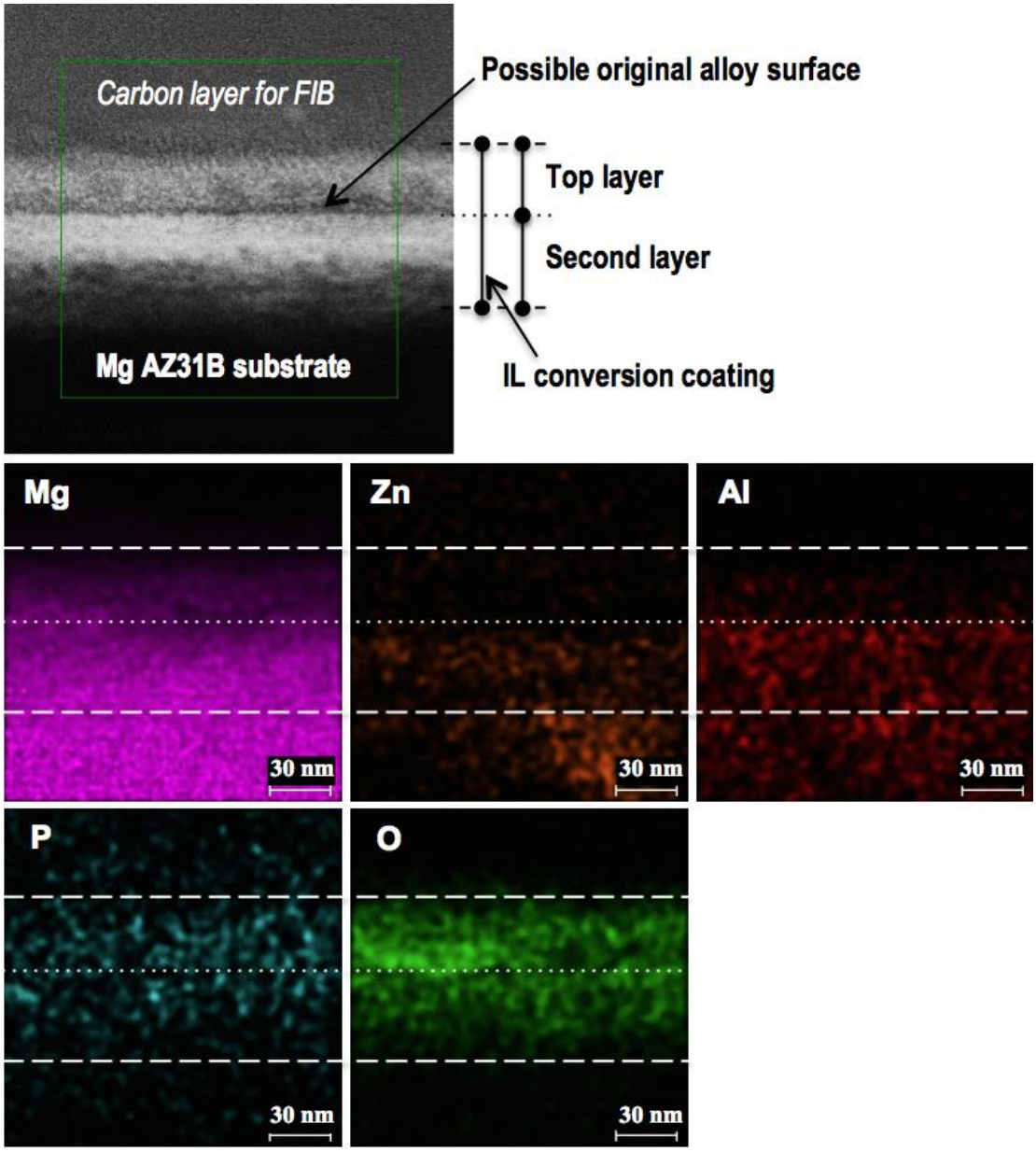

Figure 5. Cross-sectional TEM image and EDS elemental maps of the IL conversion coating on the AZ31B Mg alloy surface formed at 300 °C.

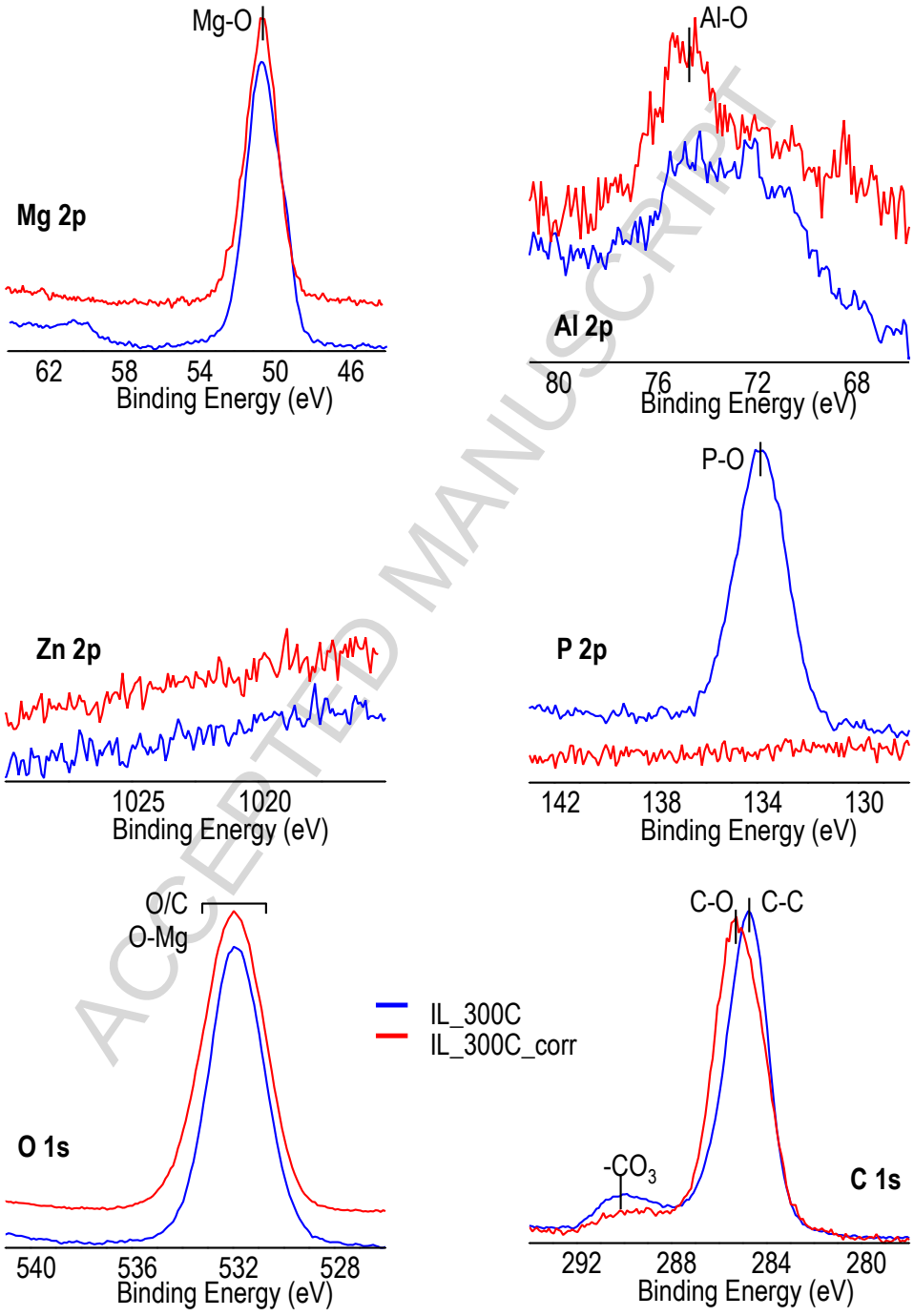

Figure 6. XPS core level spectra of IL_300C treated surfaces before (blue, IL_300C) and after (red, IL_300C_corr) the 4-hr exposure corrosion test.

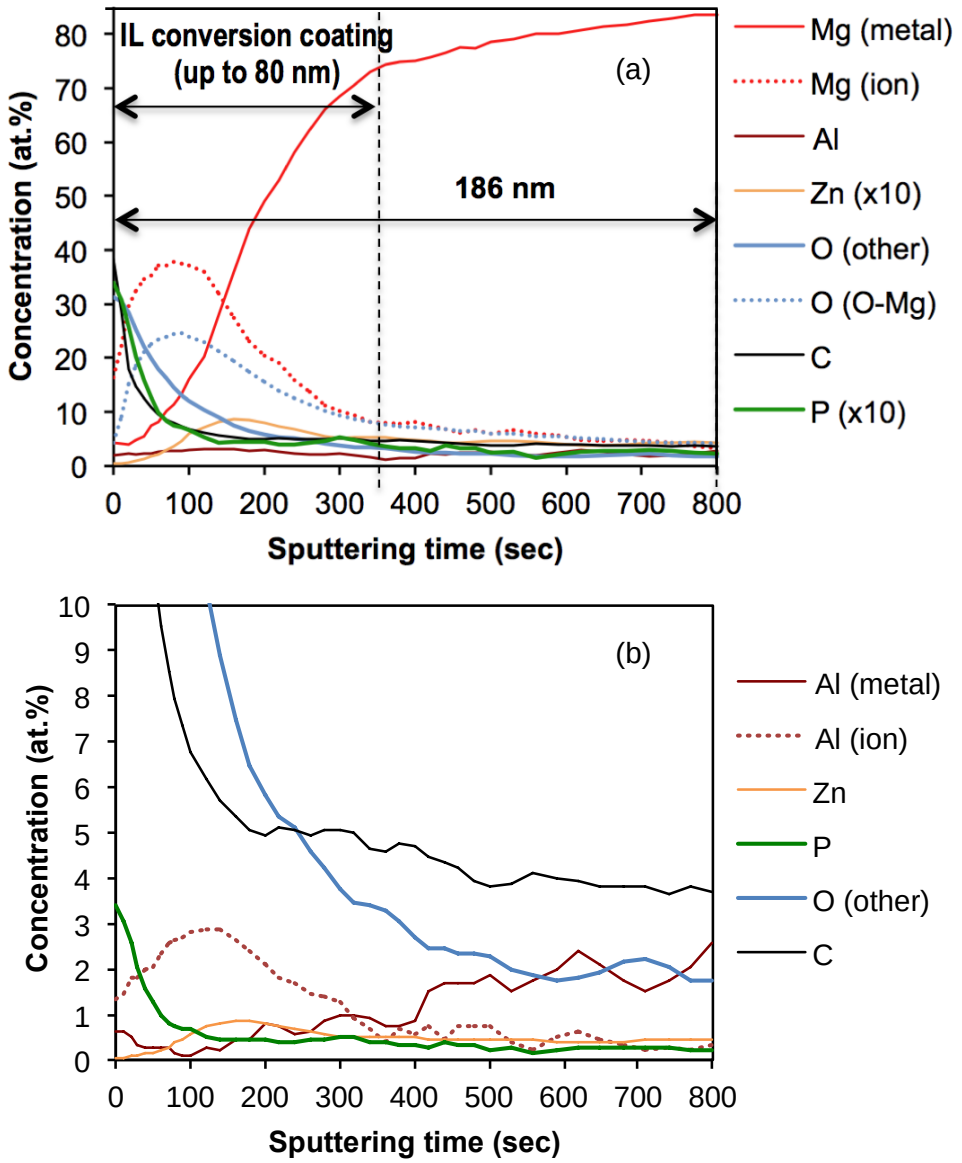

Figure 7. XPS composition depth profile of the IL_300C treated surface before corrosion testing; 7b showing the zoomed-in profiles for elements in lower concentrations.

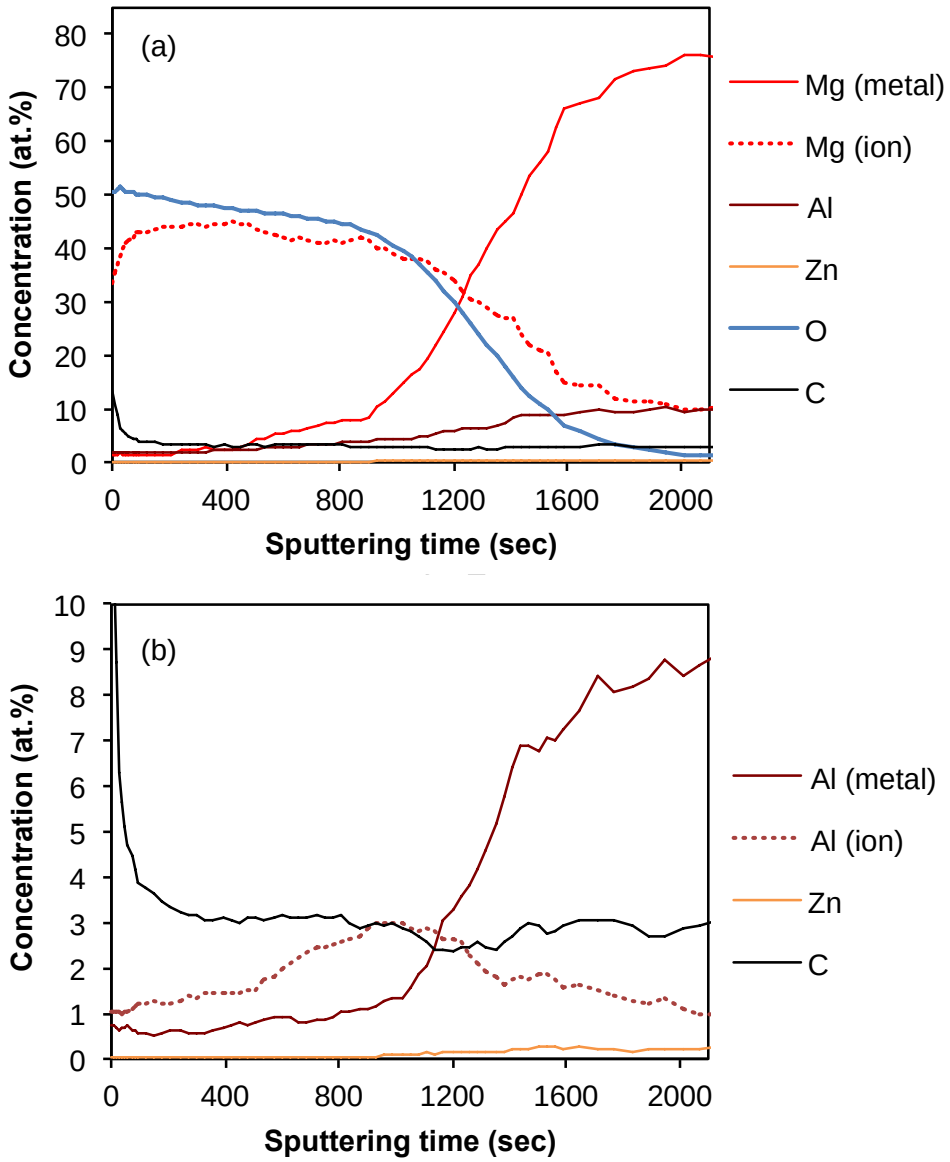

Figure 8. XPS composition depth profile of the IL_300C treated surface after the 4-hr exposure corrosion test (IL_300C_corr); 8b showing the zoomed-in profiles for elements in lower concentrations.

Highlights

1. Anti-corrosion conversion film for Mg by a protic ammonium-phosphate ionic liquid
2. No pretreatment needed and no change in surface appearance and morphology
3. The ionic liquid conversion film of 70-80 nm thick and a two-layer structure